proceedings

MDPI

Proceedings

DBD Plasma Treatment and Chitosan Layers—A Green Method for Stabilization of Silver Nanoparticles on Polyamide 6.6 †

Ana I. Ribeiro [1], Martina Modic [2], Uros Cvelbar [2], Gheorghe Dinescu [3], Bogdana Mitu [3], Anton Nikiforov [4], Christophe Leys [4], Irina Kuchakova [4], Mike De Vrieze [5], António P. Souto [1] and Andrea Zille [1,*]

[1] 2C2T-Centro de Ciência e Tecnologia Têxtil, Campus de Azurém, Universidade do Minho, 4800-058 Guimarães, Portugal; afr@2c2t.uminho.pt (A.I.R.); souto@det.uminho.pt (A.P.S.)
[2] Jožef Stefan Institute, Ljubljana, Slovenia; martina.modic@ijs.si (M.M.); uros.cvelbar@guest.arnes.si (U.C.)
[3] National Institute for Lasers, Plasma and Radiation Physics, Măgurele, Romania; dinescug@infim.ro (G.D.); mitub@infim.ro (B.M.)
[4] Department of Applied Physics, Ghent University, Ghent, Belgium; anton.nikiforov@ugent.be (A.N.); christophe.leys@UGent.be (C.L.); iryna.kuchakova@ugent.be (I.K.)
[5] Centexbel Ghent, Technologie Park 7. 9052, Ghent, Belgium; mike.devrieze@centexbel.be
* Correspondence: azille@2c2t.uminho.pt
† Presented at the First International Conference on "Green" Polymer Materials 2020, 5–25 November 2020; Available online: https://cgpm2020.sciforum.net/.

Published: 4 November 2020

Abstract: The addition of silver nanoparticles (AgNPs) to biomedical textiles can be of great interest to protect the materials against microorganisms and prevent their spread. However, the human and environmental over-exposure to AgNPs is leading to numerous concerns due to their toxicity. In this work, AgNPs were stabilized onto polyamide 6.6 fabrics (PA66) through atmospheric dielectric barrier discharge (DBD) plasma treatment and the use of chitosan (Ch) layers applied by spray. DBD plasma treatment revealed a crucial role in AgNPs adhesion (4.8 and 6.3 At%). A first layer of Ch decreased the AgNPs adhesion in both untreated and DBD plasma-treated samples but treated samples show higher concentration (1.7 and 4.1 At%). The antibacterial activity was evaluated against *Staphylococcus aureus* and *Escherichia coli* after 2 and 24 h, showing a superior action in all samples with DBD plasma treatment after 24 h. The Ch in the first layers of the composites delayed the antimicrobial action of the samples but it also may enhance antimicrobial action. The obtained coatings will allow the development of novel and safe wound dressings with improved AgNPs deposition, controlled ions released and consequently, manage the antimicrobial performance and minimize the AgNPs side effects.

Keywords: antimicrobial textiles; atmospheric plasma; green protective layers; silver nanoparticles

1. Introduction

The functionalization of biomedical textiles with silver nanoparticles (AgNPs) has received a special interest due to their unique properties namely their increased surface-to-volume ratio, that makes them potent antimicrobial agents at reduced concentrations [1]. AgNPs protect textiles against microorganisms and prevent their spread, which is extremely useful in biomedical textiles applied in case of bacterial infections, including multidrug-resistant bacteria, and healthcare-associated infections [2]. Particularly in wound dressings, textiles can act as a container or silver ions release system to prevent bacterial infections and facilitate the wound healing process [3]. The AgNPs

content in the dressings may be introduced as a coating on one or both external surfaces and/or incorporated in the fibres. In all strategies, a moist wound environment is needed to activate the release of silver ions and, therefore, induce an antimicrobial effect [4]. AgNPs are one of the most marketable nanomaterials worldwide due to their innovative and promising properties. However, with their extensive commercial use and increased production, several concerns about the human and environmental over-exposure during manufacturing, handling and disposal have emerged [5]. Some experiments were performed to understand the AgNPs toxicity to biological systems and the results showed DNA perturbations and metabolism damages in healthy cells after the exposure. AgNPs can enter in the cells by passing through biological membranes, affecting their physiology due to their small size [6]. AgNPs may cause a huge impact also in the environment due to their high surface area and reactivity. They can experience numerous transformations, difficult to predict, including oxidation or reduction, agglomeration or sedimentation, that modifies their behavior [7]. Thus, it becomes imperative to find out methods to improve the AgNPs antimicrobial effect without increasing the applied concentration and avoid their uncontrollable release to minimize or prevent the AgNPs side effects. In this work, AgNPs were stabilized onto polyamide 6.6 fabrics (PA66) through Dielectric barrier discharge (DBD) plasma treatment and the use of chitosan (Ch) layers. On the one hand, DBD plasma treatment, a low-cost and dry environmental-friendly system, can be applied to activate the surface of the fabrics promoting physical and chemical modifications. It introduces new polar functional groups and increases the surface roughness that has demonstrated to improve the AgNPs adhesion [8]. On the other hand, Ch is a biopolymer with large-scale availability, different bioactivities, biodegradable and biocompatible. It is very useful in biomedical applications, able to prevent microbial growth and promote wound healing [9,10] The main objective of this work is to obtain improved AgNPs deposition and controlled ions released. It will allow the development of novel and safe wound dressings. The combination of DBD plasma treatment and different layers of Ch makes it possible to control the amount and oxidation state of nanoparticles in the composites. Thus, it will be possible to manage the antimicrobial performance of the composites and minimize the AgNPs side effects.

2. Experiments

2.1. Materials

PA66 knitted fabric with weight per unit area of 240 g m^{-2} was selected for this study. The fabric was pre-washed with a non-ionic detergent (1 g L^{-1}) at 60 °C for 60 min., rinsed with distilled water and dried at 40 °C. Polyvinylpyrrolidone-coated AgNPs (~20 nm) were analytical grade purchased from Sigma-Aldrich, St. Louis, MO, USA and used without further purification. Chitosan at 1600 Cps (~350 MW) was obtained from Primex, Iceland.

2.2. DBD Plasma Treatment

The DBD plasma treatment was performed in a semi-industrial prototype machine (Softal GmbH/University of Minho) working at room temperature and atmospheric pressure in air, using a system of metal electrode coated with ceramic and counter electrodes coated with silicon with 50 cm effective width, gap distance fixed at 3 mm and producing the discharge at high voltage 10 kV and low frequency 40 kHz. The machine was operated at previous optimized parameters (1 kW of power and velocity of 4 m min^{-1}) [11]. The applied dosage was 5.0 kW min m^{-2}.

2.3. Composites Preparation

AgNPs was dispersed in ethanol (1 mg mL^{-1}) by a Branson 3510 ultrasonic bath (30 min) and an Optic Ivymen System CY 500 ultrasonic tip (15 min). Ch solution (0.25% (w/v)) was prepared by dissolving in acetic acid (1% (v/v)) water solution. Different composite formulations with and without DBD plasma treatment were obtained by spray in both sides of the PA66 samples (10 × 10 cm), with the system pressurized at 1.5 bar and maintained at the distance of 5 cm to the substrate. A

first layer of Ch was applied, followed by a second layer of AgNPs (Ch + AgNPs). A final protective layer was also considered (Ch + AgNPs + Ch) and samples with just AgNPs were used as control.

2.4. Scanning Electron Microscopy (SEM)

Morphological analyses of PA66 knitted fabrics were carried out with an Ultrahigh resolution Field Emission Gun Scanning Electron Microscopy (FEG-SEM), NOVA 200 Nano SEM, FEI Company (Hillsboro, OR, USA). Secondary electron images were achieved with an acceleration voltage at 5 kV. Backscattering Electron Images were performed with an acceleration voltage of 15 kV. Samples were covered with a film of Au–Pd (80–20 weight %) in a high-resolution sputter coater, 208 HR Cressington Company (Oxhey, Watford, UK), coupled to a MTM-20 Cressington High Resolution Thickness Controller.

2.5. X-Ray Photoelectron Spectroscopy (XPS)

XPS analyses were performed using a Kratos AXIS Ultra HAS (Kratos Analytical Limited, Manchester, UK), with VISION software (Vision 2, Kratos Analytical Limited, Manchester, UK) for data acquisition and CASAXPS software (casaXPS 2.3.22. Casa Software Ltd., Teignmouth, UK) for data analysis. The analysis was performed with a monochromatic Al Kα X-ray source (1486.7 eV), operating at 15 kV (150 W), in FAT (Fixed Analyser Transmission) mode, with a pass energy of 40 eV for regions ROI and 80 eV for survey. Data acquisition was performed with a pressure lower than 10-6 Pa, and it was used as a charge neutralization system. Spectra have been charge corrected to give the adventitious C1s spectral component (C-C. C-H) a binding energy of 285 eV. High-resolution spectra were collected using an analysis area of ≈1 mm^2. The peaks were constrained to have equal FWHM (Full Width at Half Maximum) to the main peak. This process has an associated error of ±0.1 eV. Spectra were analysed for elemental composition using CASAXPS software (version 2.3.15). Deconvolution into sub-peaks was performed by least-squares peak analysis software. XPSPEAK version 4.1 (Prof. Raymond W.M. Kwok, Chinese University of Hong Kong, Hong Kong, China). using the Gaussian/Lorenzian sum function and Shirley-type background subtraction. No tailing function was considered in the peak fitting procedure. The components of the various spectra were mainly modelled as symmetrical Gaussian peaks unless a certain degree of Lorentzian shape was necessary for the best fit. The best mixture of Gaussian-Lorentzian components was defined based on the instrument and resolution (pass energy) settings used as well as the natural line width of the specific core hole.

2.6. Antimicrobial Analyses

The antibacterial efficacy of the PA66 composites was measured quantitatively according to the standard shake flask method (ASTM-E2149-01). Gram-positive and Gram-negative bacteria were used. *Staphylococcus aureus* (*S. aureus*, ATCC 6538) and *Escherichia coli* (*E. coli*, ATCC 25922), respectively. The experiment was conducted aseptically to ensure the absence of any contamination. Bacteria inoculum were prepared from a single colony and incubated overnight in tryptic soy broth (TSB, Merck) at 37 °C and 120 rpm. Each test was carried out using an initial concentration of 1.5–3.0 × 10^7 CFUs/mL in PBS. PA66 samples of 0.05 g weight were incubated in 5 mL of bacteria suspension at 37 °C and 100 rpm. Before contact with samples (0 h) and after contact with samples (24 h), the bacteria were serially diluted, cultured onto tryptic soy agar (TSA, Merck) plates, and further incubated for 24 h. The results were obtained by counting the colonies of surviving bacteria on the agar plates. Antimicrobial activity was reported in terms of log reduction, calculated as the ratio between the number of surviving bacteria colonies present on the TSA plates. before and after contact with the samples. All antimicrobial experiments were conducted in triplicate.

3. Results

Novel composites were produced using chitosan (Ch) to stabilize AgNPs onto untreated and DBD plasma treated polyamide. The different formulations were obtained by spray where a first

layer of Ch was applied, followed by a second layer of nanoparticles dispersed in ethanol (Ch + NPs). A final protective layer was also considered (Ch + NPs + Ch) and samples with just NPs were used as control.

3.1. SEM

SEM analyses of PA66 untreated and DBD plasma-treated composites were employed to evaluate the distribution and the aglomeration of AgNPs deposited into the samples, and also to confirm the allocation of the final Ch protection layer (Figure 1). The low magnification was applied to analyze the AgNPs distribution (1000×) and a higher magnification was used to assess the nanoparticles aglomeration and the Ch layers (5000×).

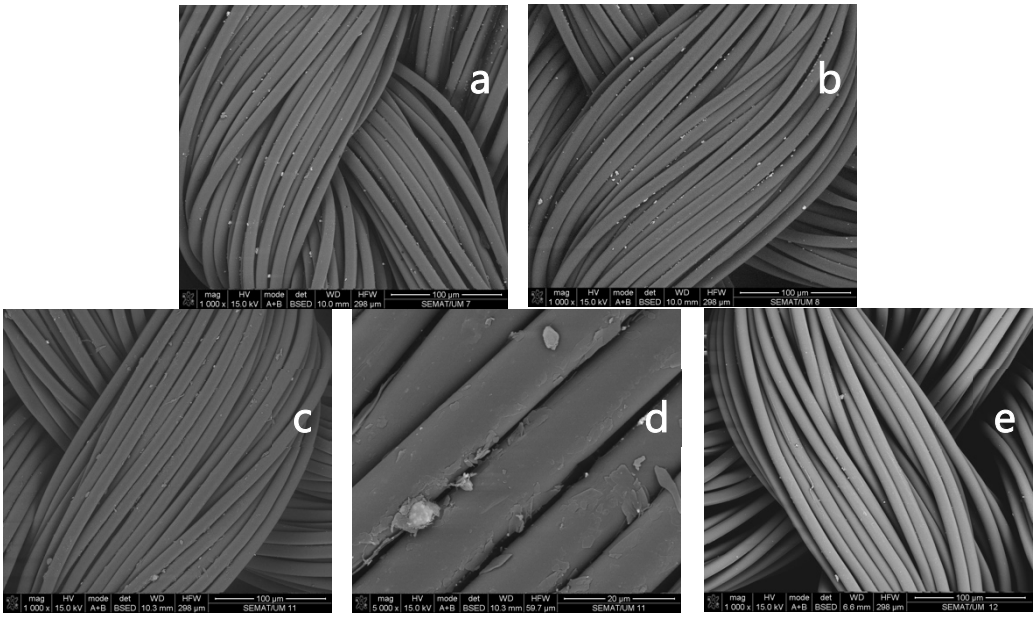

Figure 1. SEM images of untreated (**a**,**c**,**d**) and DBD plasma treated (**b**,**e**) of control samples (**a**,**b**) and Ch + AgNPs + Ch composites (**c**–**e**) with magnification of 1000× (**a**–**c**,**e**) and 5000× (**d**).

3.2. XPS

XPS analysis was carried out to compare the surface atomic percentage of oxygen, carbon, nitrogen and silver in the composites, and calculate the respective atomic ratios (O/C and N/C) (Table 1). The chemical modifications of composites by DBD plasma treatment and Ch layers were evaluated by the chemical bonding information. This data was obtained by the deconvolution spectra of C1s, N1s, O1s, and Ag3d (Tables 2 and 3).

Table 1. Relative chemical composition of untreated (UT) and DBD plasma-treated (DBD) PA66 samples.

Samples	C (At%)	O (At%)	N (At%)	Ag (At%)	O/C Ratio	N/C Ratio
AgNPs UT	61.7	21.5	11.9	4.8	0.3	0.2
AgNPs DBD	58.4	24.1	11.2	6.3	0.4	0.2
Ch + AgNPs UT	61.6	25.2	11.5	1.7	0.4	0.2
Ch + AgNPs DBD	55.4	32.0	8.5	4.1	0.6	0.2
Ch + AgNPs + Ch UT	62.0	23.5	11.0	3.4	0.4	0.2
Ch + AgNPs + Ch DBD	53.6	31.9	11.2	3.4	0.6	0.2

Table 2. Deconvolution analysis of the C1s and O1s peaks for the untreated (UT) and DBD plasma-treated (DBD) PA66 samples (SD ± 0.3 eV), results are presented as a percentage of relative area.

Samples	C1s					O1s		
	283.2 eV	285.0 eV	286.3 eV	287.9 eV	289.3 eV	531.4 eV	533.0 eV	533.9 eV
AgNPs UT	-	70.8	15.8	13.4	-	71.4	22.7	5.9
AgNPs DBD	-	67.9	16.8	13.4	1.9	61.2	28.8	10.0
Ch + AgNPs UT	-	66.8	19.0	14.1	-	64.0	28.6	7.4
Ch + AgNPs DBD	1.3	52.2	25.5	17.0	4.1	43.1	43.3	13.6
Ch + AgNPs + Ch UT	-	70.2	17.5	12.3	-	62.8	30.4	6.7
Ch + AgNPs + Ch DBD	1.5	55.1	24.0	16.9	2.4	50.2	42.2	7.6

Table 3. Deconvolution analysis of the N1s and Ag3d peaks for the untreated (UT) and DBD plasma-treated (DBD) PA66 samples (SD ± 0.3 eV), results are presented as a percentage of relative area.

Samples	N1s			Ag3d			
	399.8 eV	400.4 eV	401.4 eV	368.3 eV	370.0 eV	374.6 eV	376.0 eV
AgNPs UT	89.8	-	10.2	53.1	14.3	32.6	-
AgNPs DBD	87.1	-	12.9	43.5	15.3	27.8	13.4
Ch + AgNPs UT	79.8	13.1	7.1	46.3	-	53.7	-
Ch + AgNPs DBD	56.1	31.0	12.9	45.7	12.9	23.9	17.5
Ch + AgNPs + Ch UT	81.8	10.9	7.2	35.9	17.8	32.4	13.9
Ch + AgNPs + Ch DBD	47.7	40.6	11.7	41.7	13.8	35.3	9.2

3.3. Antimicrobial Analyses

The quantitative antibacterial activity was evaluated against *S. aureus* and *E. coli* after 2 and 24 h by shake flask method (Figure 2).

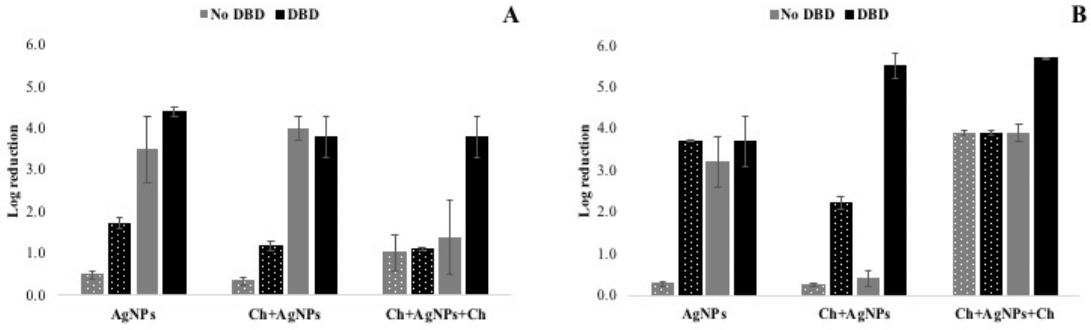

Figure 2. Antimicrobial action of untreated and DBD-plasma treated samples with AgNPs and different layers of Ch against S. aureus (**A**) and E. coli (**B**) after 2 h (dotted fill) and 24 h (solid fill).

4. Discussion

4.1. SEM

SEM images confirmed the presence of AgNPs uniformly distributed in both DBD plasma-treated and untreated analyzed samples but it was not possible to validate if DBD plasma treatment

enhanced the AgNPs deposition rates on the fabric's surface (Figure 1). Thus, the chemical composition was calculated in XPS analysis and will be discussed in the respective section. The collected images also showed some nanoparticles agglomeration in all samples, independently if the AgNPs are deposited directly in the fabric samples or after the first layer of chitosan. These results suggest that with the AgNPs deposition by spray, the agglomeration was independent of the DBD plasma treatment and chitosan layer, it is only related to the initial AgNPs dispersion in ethanol. Previous DLS studies showed that 20 nm polyvinylpyrrolidone-coated AgNPs ethanol dispersions, at the same concentration, present some agglomeration with an average size of 281.0 ± 1.5 nm [12]. The final chitosan layer is clearly visible mainly when the higher magnification is applied (Figure 1d). The exposure of AgNPs decreased but the coating is not completely uniform. Upcoming studies may be planned to reduce the nanoparticles agglomeration and improve the chitosan final layer.

4.2. XPS

The relative chemical composition of C, N, O and Ag in PA66 composites and control samples were calculated using XPS results (Table 1). DBD plasma treatment revealed a crucial role in nanoparticles adhesion, 4.8 and 6.3 At% in control samples. The first layer of Ch decreased the nanoparticles adhesion in both untreated and DBD plasma-treated samples but treated samples showed higher concentration (1.7 and 4.1 At%). DBD plasma-treated samples displayed an increase in oxygen content and O/C ratio (Table 1). This difference was even more evident in samples with Ch layers. Thus, the results confirmed the integration of oxygen species from the air during the plasma treatment (21.5 and 24.1 At% for control samples). In addition to the superior AgNPs adhesion in DBD plasma treated samples, also superior adsorption of chitosan in DBD plasma-treated was observed (for Ch+AgNPs samples, 25.2 and 32.0 At%). DBD plasma treatment is able to change the surface properties of PA66 fabrics, providing more roughness surfaces and newly reactive oxygen species [13]. The deconvolution spectra of C1s, N1s, O1s, and Ag3d highlighted the chemical modifications of PA66 surface due to DBD plasma treatment and chitosan layers (Tables 2 and 3). The C1s envelopes of untreated samples presented the usual three peaks at 285.0, 286.3 and 287.9 eV attributed to C-C/C-H, C-N and O=C-N bonds, respectively [14]. DBD plasma-treated samples showed the same peaks and another new peak at 289.3 eV attributed to O-C=O bonds, evidencing the introduction of novel oxygen species by DBD plasma treatment [15]. PA66 composites with both DBD plasma treatment and Ch layers showed an additional minor peak at 283.2 eV attributed to C-C/C=C bonds due to the interactios between silver ions and chitosan hydrocarbons [12,16,17]. The O1s spectra showed three peaks attributed to O=C (531.4 eV), HO–C bonds (533.0 eV) and O-C=O (533.9 eV). The peak at 531.4 eV was prevalent in all composites. However, after DBD plasma-treatment, this peak decreased and the other oxygen peaks increased, suggesting a strong PA66 surface oxidation. The N1s region deconvolution, in control samples presented two peaks at 399.8 and 401.4 eV, attributed to N-C and N-H, respectively [18–20]. The composites with chitosan presented an extra peak at 400.4 eV corresponding to amine groups of chitosan [21]. These deconvolutions proved the superior adhesion of chitosan in DBD plasma-treated samples. The Ag3d deconvolution spectra showed the oxidation states of AgNPs in the different formulations. Two doublets appeared, one attributed to metal silver at 368.3 (Ag 3d5/2) and 374.6 eV (Ag 3d3/2) and other attributed to ionic silver in AgNPs surface at 370.0 and 376.0 eV [22,23]. The intensity of the second doublet was superior in DBD plasma-treated control and Ch + AgNPs samples, indicating a superior AgNPs oxidation in these samples. Interestingly, when a final layer of chitosan is applied (Ch + AgNPs samples), DBD plasma treatment did not influence the oxidation state of AgNPs and the second doublet did not increase, suggesting that chitosan operated as a coating to protect the AgNPs from oxidation.

4.3. Antimicrobial Analyses

The antibacterial activity was evaluated against *S. aureus* and *E. coli* after 2 and 24 h (Figure 2). The results showed to be according to AgNPs oxidation state and chitosan concentration. For *S. aureus*, DBD plasma treatment and the Ch in the first layer of the composite delayed the antimicrobial action that can be related to the superior adhesion of chitosan in these samples. After 24 h, treated

samples showed better or equivalent results, showing suitable properties to control the antimicrobial action during this period. For *E. coli*, all DBD plasma-treated samples showed a superior action. Just the first layer of chitosan was able to delay the antimicrobial action. When the final layer of chitosan was applied, the antimicrobial action increases even after 2 h. In some cases, the final Ch layer enhances the antimicrobial action of the composites.

5. Conclusions

This study showed the potential of DBD plasma treatment to improve or control the antimicrobial action of composites treated with this technology. Depending on the composite formulation, it was possible to perform a rapid antimicrobial action or control it. It demonstrated to be a suitable method to improve the adhesion of both AgNPs and chitosan. Some future experiments must be performed to improve the uniformity of chitosan deposited layers, decrease the AgNPs agglomeration and decrease the AgNPs concentration. The obtained coatings can be used for the development of novel and safe wound dressings with improved properties.

Author Contributions: A.I.R. wrote the manuscript, performed the main analysis and data collection. M.D.V. G.D., B.M. and A.P.S. performed data interpretation. M.M. and U.C. performed and interpreted the antimicrobial analysis. A.N., C.L. and I.K. performed the XPS data analysis and deconvolutions. A.Z. supervised all works and finalized the manuscript. All authors have read and agreed to the published version of the manuscript.

Acknowledgments: This work was funded by FEDER funds through the Operational Competitiveness Program-COMPETE and by National Funds through Fundação para a Ciência e Tecnologia (FCT) under the project POCI-01-0145-FEDER-007136 and UID/CTM/00264/2019. A. I. Ribeiro acknowledges FCT, Portugal, for its doctoral grant financial support (SFRH/BD/137668/2018). A. Zille also acknowledges financial support of the FCT project PTDC/CTM-TEX/28295/2017 financed by FCT, FEDER and POCI.

Conflicts of Interest: The authors declare no conflict of interest.

References

1. Mihai, M.M.; Dima, M.B.; Dima, B.; Holban, A.M. Nanomaterials for Wound Healing and Infection Control. *Materials* **2019**, *12*, 2176, doi:10.3390/ma12132176.
2. Ballottin, D.; Fulaz, S.; Cabrini, F.; Tsukamoto, J.; Durán, N.; Alves, O.L.; Tasic, L. Antimicrobial textiles: Biogenic silver nanoparticles against Candida and Xanthomonas. *Mater. Sci. Eng. C* **2017**, *75*, 582–589, doi:10.1016/j.msec.2017.02.110.
3. Kalantari, K.; Mostafavi, E.; Afifi, A.M.; Izadiyan, Z.; Jahangirian, H.; Rafiee-Moghaddam, R.; Webster, T.J. Wound dressings functionalized with silver nanoparticles: Promises and pitfalls. *Nanoscale* **2020**, *12*, 2268–2291, doi:10.1039/c9nr08234d.
4. Boateng, J.; Catanzano, O. Silver and Silver Nanoparticle-Based Antimicrobial Dressings. *Ther. Dress. Wound Heal. Appl.* **2020**, 157–184, doi:10.1002/9781119433316.ch8.
5. Weldon, B.A.; Faustman, E.M.; Oberdörster, G.; Workman, T.; Griffith, W.C.; Kneuer, C.; Yu, I.J. Occupational exposure limit for silver nanoparticles: Considerations on the derivation of a general health-based value. *Nanotoxicology* **2016**, *10*, 945–956, doi:10.3109/17435390.2016.1148793.
6. Ema, M.; Okuda, H.; Gamo, M.; Honda, K. A review of reproductive and developmental toxicity of silver nanoparticles in laboratory animals. *Reprod. Toxicol.* **2017**, *67*, 149–164, doi:10.1016/j.reprotox.2017.01.005.
7. León-Silva, S.; Fernández-Luqueño, F.; López-Valdez, F. Silver Nanoparticles (AgNP) in the Environment: A Review of Potential Risks on Human and Environmental Health. *Water Air Soil Pollut.* **2016**, *227*, 306, doi:10.1007/s11270-016-3022-9.
8. Ribeiro, A.I.; Senturk, D.; Silva, K.S.; Modic, M.; Cvelbar, U.; Dinescu, G.; Mitu, B.; Nikiforov, A.; Leys, C.; Kuchakova, I.; et al. Efficient silver nanoparticles deposition method on DBD plasma-treated polyamide 6,6 for antimicrobial textiles. *IOP Conf. Ser. Mater. Sci. Eng.* **2018**, *460*, 460, doi:10.1088/1757-899x/460/1/012007.
9. Shao, W.; Wu, J.; Wang, S.; Huang, M.; Liu, X.; Zhang, R. Construction of silver sulfadiazine loaded chitosan composite sponges as potential wound dressings. *Carbohydr. Polym.* **2017**, *157*, 1963–1970, doi:10.1016/j.carbpol.2016.11.087.

10. Nešović, K.; Janković, A.; Radetić, T.; Vukašinović-Sekulić, M.; Kojić, V.; Živković, L.; Perić-Grujić, A.; Rhee, K.Y.; Mišković-Stanković, V. Chitosan-based hydrogel wound dressings with electrochemically incorporated silver nanoparticles—In vitro study. *Eur. Polym. J.* **2019**, *121*, 109257, doi:10.1016/j.eurpolymj.2019.109257.
11. Oliveira, F.R.; Souto, A.P.; Carneiro, N.; Nascimento, J. Surface Modification on Polyamide 6.6 with Double Barrier Discharge (DBD) Plasma to Optimise Dyeing Process by Direct Dyes. *Mater. Sci. Forum* **2010**, *636–637*, 846–852, doi:10.4028/www.scientific.net/msf.636-637.846.
12. Ribeiro, A.I.; Modic, M.; Cvelbar, U.; Dinescu, G.; Mitu, B.; Nikiforov, A.; Leys, C.; Kuchakova, I.; De Vrieze, M.; Felgueiras, H.P.; et al. Effect of Dispersion Solvent on the Deposition of PVP-Silver Nanoparticles onto DBD Plasma-Treated Polyamide 6,6 Fabric and Its Antimicrobial Efficiency. *Nanomaterials* **2020**, *10*, 607, doi:10.3390/nano10040607.
13. Ribeiro, A.I.; Modic, M.; Cvelbar, U.; Dinescu, G.; Mitu, B.; Nikiforov, A.; Leys, C.; Kuchakova, I.; Souto, A.P.; Zille, A. Atmospheric-Pressure Plasma Spray Deposition of Silver/HMDSO Nanocomposite on Polyamide 6,6 with Controllable Antibacterial Activity. *AATCC J. Res.* **2020**, *7*, 1–6, doi:10.14504/ajr.7.3.1.
14. Ribeiro, A.I.; Senturk, D.; Silva, K.K.D.O.S.; Modic, M.; Cvelbar, U.; Dinescu, G.; Mitu, B.; Nikiforov, A.; Leys, C.; Kuchakova, I.; et al. Antimicrobial Efficacy of Low Concentration PVP-Silver Nanoparticles Deposited on DBD Plasma-Treated Polyamide 6,6 Fabric. *Coatings* **2019**, *9*, 581, doi:10.3390/coatings9090581.
15. Manakhov, A.M.; Michlíček, M.; Felten, A.; Pireaux, J.-J.; Nečas, D.; Zajíčková, L. XPS depth profiling of derivatized amine and anhydride plasma polymers: Evidence of limitations of the derivatization approach. *Appl. Surf. Sci.* **2017**, *394*, 578–585, doi:10.1016/j.apsusc.2016.10.099.
16. Huang, G.; Mo, L.Q.; Wei, Y.X.; Zhou, H.; Guo, Y.A.; Wei, S.J. Effect of Mesoporous Chitosan Action and Coordination on the Catalytic Activity of Mesoporous Chitosan-Grafted Cobalt Tetrakis (p-Sulfophenyl) Porphyrin for Ethylbenzene Oxidation. *Catalysts* **2018**, *8*, 199, doi:10.3390/catal8050199.
17. Fouda, A.; Salem, S.S.; Wassel, A.R.; Hamza, M.F.; Shaheen, T. Optimization of green biosynthesized visible light active CuO/ZnO nano-photocatalysts for the degradation of organic methylene blue dye. *Heliyon* **2020**, *6*, doi:10.1016/j.heliyon.2020.e04896.
18. Khorshidi, B.; Thundat, T.; Fleck, B.A.; Sadrzadeh, M. A Novel Approach Toward Fabrication of High Performance Thin Film Composite Polyamide Membranes. *Sci. Rep.* **2016**, *6*, 22069, doi:10.1038/srep22069.
19. Wang, C.; Li, Z.; Chen, J.; Zhong, Y.; Ren, L.; Pu, Y.; Dong, Z.; Wu, H. Influence of blending zwitterionic functionalized titanium nanotubes on flux and anti-fouling performance of polyamide nanofiltration membranes. *J. Mater. Sci.* **2018**, *53*, 10499–10512, doi:10.1007/s10853-018-2288-2.
20. Moles, M.D.; Scotchford, C.A.; Ritchie, A.C. Oxidation State of a Polyurethane Membrane after Plasma Etching. *Conf. Pap. Sci.* **2014**, *2014*, 1–11, doi:10.1155/2014/347979.
21. Silva; Ladchumananandasivam, R.; Nascimento, J.H.O.; Oliveira, F.R.; Souto, A.P.; Felgueiras, H.P.; Zille, A. Multifunctional Chitosan/Gold Nanoparticles Coatings for Biomedical Textiles. *Nanomaterials* **2019**, *9*, 1064, doi:10.3390/nano9081064.
22. Mirzaei, A.; Janghorban, K.; Hashemi, B.; Bonyani, M.; Leonardi, S.G.; Neri, G. Characterization and optical studies of PVP-capped silver nanoparticles. *J. Nanostructure Chem.* **2016**, *7*, 37–46, doi:10.1007/s40097-016-0212-3.
23. Pagliai, M.; Muniz-Miranda, M.; Schettino, V.; Muniz-Miranda, M. Competitive Solvation and Chemisorption in Silver Colloidal Suspensions. In *UK Colloids 2011*; Springer Science and Business Media LLC: Berlin/Heidelberg, Germany, 2012; pp. 39–44.